Atomic multiplets at the $L_{2,3}$ edge of 3d transition metals and the ligand K edge in x-ray absorption spectroscopy of ionic systems

P. Olalde-Velasco,[1,*] J. Jiménez-Mier,[2,†] J. Denlinger,[1] and W.-L. Yang[1]

[1]*The Advanced Light Source, Lawrence Berkeley National Laboratory, Berkeley, California 94720, USA*

[2]*Instituto de Ciencias Nucleares, UNAM, Circuito Exterior, Ciudad Universitaria, 04510 México D.F., México*

(Received 12 September 2012; published 28 June 2013)

Experimental X-ray absorption spectra at the fluorine K and transition metal $L_{2,3}$ absorption edges of the MF_2 (M = Cr-Ni) family are presented. Ligand field calculations in D_{4h} symmetry show very good agreement with the transition metal $L_{2,3}$ XAS spectra. To successfully explain nominal Cr^{2+} $L_{2,3}$ XAS spectrum in CrF_2, the inclusion of Cr^{+} and Cr^{3+} was needed implying the presence of a disproportionation reaction. The multiplet calculations were then modified to remove the structure of the 2p hole in the calculated M 2p $\rightarrow$ 3d absorption spectra. These results for the $3d^{n+1}$ states are in one to one correspondence with the leading edge structures found at the fluorine K edge. A direct comparison with the metal $L_{2,3}$ edges also indicates that there is evidence of the metal multiplet at the fluorine K pre-edge structures.

DOI: 10.1103/PhysRevB.87.245136 PACS number(s): 71.20.−b, 71.27.+a, 78.70.Dm

I. INTRODUCTION

Transition metal (TM) compounds display varied interesting properties as a consequence of the interplay of structure, charge distribution, and electronic correlations in 3d electrons. Because of possible technological applications transition metal oxides (TMOs) have been dominating the study of TM compounds. Among TM compounds, the difluorides are the most ionic and therefore provide an excellent test ground for understanding ionic bonding. As in the case of TM monoxides in the TM difluorides (rutile structure) the cation is under the influence of a cubic crystal field. It is common to assume that the bonding in oxides and halides occurs between TM 4s, 4p states and ligand 2p states forming the valence band and empty antibonding combinations. The role of TM 3d electrons is also antibonding in nature.[1,2] Later, by influence of the cubic crystal fields exerted by the ligands surrounding the cation, the 3d orbitals unfold into t_{2g} and e_g sub-bands,[1] which may further split in spin-up and spin-down sub-bands[3] due to exchange interaction. The relative ordering among them depends on the relative magnitude of both exchange and crystal field splitting.[3,4]

The element specificity and orbital selectivity of x-rays allows us to probe unoccupied F2p and M3d states through 1s $\rightarrow$ 2p and 2p $\rightarrow$ 3d transitions, respectively.[1] In this sense, the unoccupied TM 3d states of the MF_2 have been studied by x-ray absorption spectroscopy (XAS) at the TM $L_{2,3}$ edges (2p $\rightarrow$ 3d transition).[5–11] It has been demonstrated that these metal XAS spectra can be understood in terms of ligand field atomic multiplet calculations (LFM).[5,7–15] However, up to date there is no high resolution study available that encompasses systematically all the metals in this family of compounds. On the other hand, the unoccupied F 2p states in the TM difluorides have been measured by probing the F-K edge through 1s $\rightarrow$ 2p transitions.[4–6,16,17] These spectra have been interpreted in terms of the consecutive filling of t_{2g} $\uparrow$, t_{2g} $\downarrow$, e_g $\uparrow$, and e_g $\downarrow$ sub-bands[4] as well as in terms of spin polarized molecular-orbital calculations.[16] From the experience on TMOs[1–3,15,18] it is known that the ligand K edge spectra agree quite well with DFT calculations of the ligand 2p density of states (DOS), although usually a shift must be applied to account for the core hole potential created during the x-ray absorption process and the polarization effect of the extra electron in the p band. The good agreement is mainly due to the lack of spin orbit coupling in the 1s $\rightarrow$ 2p transition and the fact that 2p electrons are delocalized.

Additional information regarding the electronic structure of the TM difluorides have been obtained experimentally from photoelectron spectroscopies (PES)[1,19] and x-ray emission spectroscopy (XES).[16,20,21] From theory, scattered LDA[22,23] and Hartree-Fock[24] calculations are available. Recently, we have achieved a complete experimental picture on the electronic structure evolution of MF_2 through a combined study of XAS and XES.[25] From all these works it is clear that there is significant hybridization of F2p-TM3d states around the Fermi level. Particularly, although there is evidence that TMs are responsible for the structures in the leading edges of the O-K edge in TMOs[2,3,15,18,26] as well as in Cl K edges of organo-titanium compounds,[27] it has been argued that multiplet effects are not as evident in the ligand K edges as they are in the TM L edges.[1]

In this work we demonstrate that in the MF_2 ionic systems the structures displayed in the FK leading edges of the XAS spectra contain atomic multiplet effects from the TM 3d states. To accomplish this, we first reproduce the experimental metal $L_{2,3}$ absorption spectra using ligand field multiplet (LFM) calculations. The calculations are then modified to remove the changes in the multiplet absorption spectra introduced by the structure of the 2p hole. One therefore obtains the structure of the metal 3d shell with an extra 3d electron. These $3d^{n+1}$ absorption spectra with a "structureless hole" are then shifted to compare them with the leading edge features observed at the fluorine K edge. This approach is used to investigate F2p-M3d hybridization features on the F-K XAS spectra by accounting for an extra electron interacting in the 3d band that originates from the 1s $\rightarrow$ 2p transition. These $3d^{n+1}$ configurations are an alternative approximation to describe the upper-Hubbard band (UHB) for each difluoride.[25] In general, this procedure allows a direct identification of a number of structures in the F-K pre-edge, with a good indication of their

 ©2013 American Physical Society

energy separation. Interestingly, equivalent information can be obtained by directly aligning the structures appearing in the F-K spectra to those at the L_2 and L_3 experimental edges of the TM for each difluoride. Signature of multiplet effects in F-K spectra is proposed to appear as a combined effect of the strong ionic character of the MF_2 bonding, the high ligand to metal charge transfer (LMCT) energies involved (about 3 eV larger than in oxides),[25,28] the narrowing of the F band as compared to O, and hybridization. This aligning procedure of F2p-TM3d bands can be used to unambiguously identify hybridization features in ionic systems. On the other hand, evidence of a disproportionation reaction driven by exchange correlations inducing a negative effective U is identified in CrF_2.[28,29]

The paper is organized as follows: First we discuss the experimental conditions under which the XAS spectra of both F-K and M-L edges were acquired. Then we discuss the fundamentals of our atomic LFM calculations that explain the structures of TM $L_{2,3}$ XAS and our $3d^{n+1}$ calculations with a "2p structureless" hole. We clarify in a definitive way a long standing issue on the origin of structures in the nominal Cr^{2+} spectrum in CrF_2,[9] namely the presence of Cr^{+}, Cr^{2+}, and Cr^{3+} oxidation states. Later we present the F-K XAS spectra and compare them with (i) the corresponding TM3d^{n+1} structureless 2p hole calculations, and (ii) experimental TM $L_{2,3}$ edges. From here signature of TM 2p-3d multiplet structure on the F-K XAS spectra is demonstrated.

II. EXPERIMENTS

The XAS measurements were made at beamline 8.0.1 of the Advanced Light Source at the Lawrence Berkeley National Laboratory.[30] The samples were commercially available fresh polycrystalline powders (Sigma-Aldrich) with purity greater than 99.9%. The fluorine K edge spectra were all collected in one experimental run at room temperature. The data at the transition metal L edges were obtained at separate runs for each sample. The XAS experiments were performed in ultra high vacuum (UHV) conditions with the typical pressure inside the acquisition chamber in the low 10^{-9} Torr range. All the XAS spectra were collected in the total electron yield (TEY) mode by registering the sample current as the incoming radiation was scanned and the data were normalized to the photon flux. There is ambiguity in the reported XAS spectra of Fe[5–7,17] and Cr,[7,9] which we found to be the more susceptible to oxidation. In the case of FeF_2 we observed an increase in intensity of the structure at 709 eV in samples exposed to air. For this reason Fe spectra were collected in two separate runs with different fresh samples, and we found that our measurements are consistent and in agreement with those of Chen and Sette.[7] On the other hand, as we will demonstrate further, our CrF_2 sample is more oxidized as compared with others reported in literature.[7,9]

III. CALCULATIONS

Atomic multiplet calculations including ligand field effects (LFM) in D_{4h} symmetry were performed to reproduce metal $L_{2,3}$ edges XAS spectra.[1] The ligand field parameters 10Dq, Ds, and Dt, the contraction factor for the atomic Slater integrals, and the monochromator width were all varied until we found the best agreement with measured metal XAS L edges. The Slater integrals are contracted in order to account for a certain degree of intra-atomic correlation.[1] Values for the $2p_j$ core hole widths required to perform the calculations were taken directly from the article by Krause and Olivier.[31] Our approach successfully accounts for the main structures in the spectra (see Fig. 1). This is true even for the Jahn-Teller distorted CrF_2 which is definitely a D_{4h} symmetry system.[9] The reason for this is that Cr^{2+} is in d^4 configuration and the effect of the crystal field implies an elongation of the Cr-F bonding along the z axis in order to break the degeneracy of the e_g orbitals.[9] The values of the parameters from our best fits for MnF_2 to NiF_2 are given in Table I. Our 10Dq and the contraction of the Slater integrals are close to those reported for TM^{2+} ions in O_h symmetry.[12] This implies that deviation from O_h symmetry is small.

For CrF_2 three ionic states, namely Cr^{+}, Cr^{2+}, and Cr^{3+}, were included in the calculation. This allows for the possibility

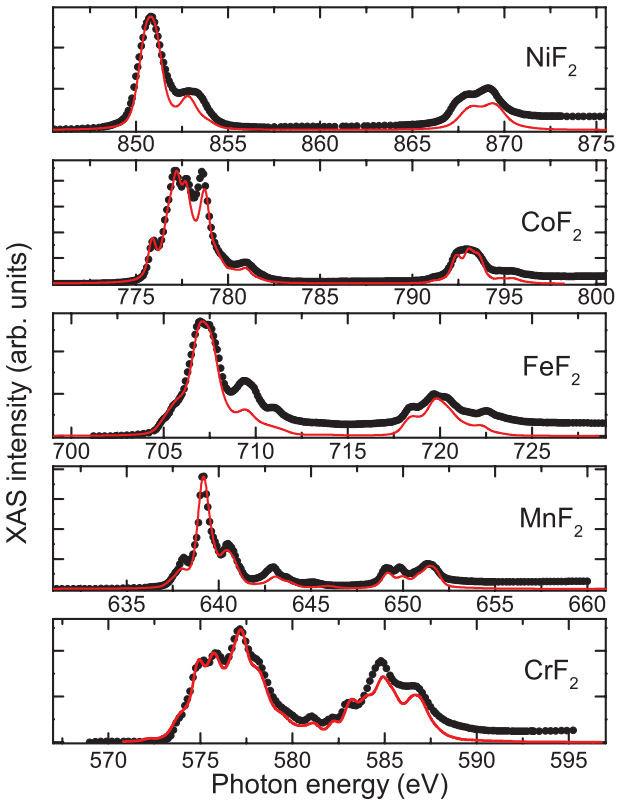

FIG. 1. (Color online) Comparison between the experimental $2p \rightarrow 3d$ x-ray absorption spectra (bullets) and the atomic multiplet absorption spectra (solid line) for the MF_2 compounds.

TABLE I. Parameters used in the atomic multiplet calculation for MF_2 XAS. For CrF_2 see Table II.

Metal	Mn	Fe	Co	Ni
10Dq (eV)	0.64	0.92	0.70	1.55
Ds (eV)	−0.01	−0.16	−0.12	0.12
Dt (eV)	−0.04	−0.02	−0.02	0.03
Slater contraction	0.83	0.75	0.80	0.80
Monochromator width (eV)	0.34	0.54	0.24	0.56

TABLE II. Parameters used in the CrF_2 spectra calculation.

Parameter	Cr^+	Cr^{2+}	Cr^{3+}
10Dq (eV)	0.80	0.85	0.80
Ds (eV)	0	0.17	−0.20
Dt (eV)	0	−0.07	0.20
Coefficient (this work)	0.17	0.35	0.47
Coefficient (spectrum in Ref. 9)	0.24	0.38	0.38

of sample oxidation and/or disproportionation. The resulting spectrum is then the linear superposition of the individual spectra that gives the best agreement with experiment. Because the calculated spectra are normalized to the number of $3d$ holes, the superposition coefficients directly give the ratio of that ionic state present in the sample.[32] To simplify the choice of parameters for Cr^+ we only used the octahedral ligand field energy 10Dq. For the other two ionic states we also included the Ds and Dt parameters in D_{4h} symmetry.[1] The individual spectra were calculated using a 0.80 contraction factor for the Slater integrals, the same values for the $2p$ hole width,[31] and a monochromator half width at half maximum of 0.20 eV. The coefficients for the linear superposition were then chosen to achieve the best agreement with the experimental data. We found that by using the same set of absorption spectra, but with different values of the linear superposition coefficients and monochromator width, we were able to achieve a very good fit for the spectra of the less oxidized CrF_2 sample shown in Ref. 9. The values of the ligand field parameters and the coefficients used in the calculation are given in Table II. The O_h ligand field energy 10Dq is nearly equal for all oxidation states and the D_{4h} parameters are by no means as large as the ones used by Theil *et al.* in their analysis.

It has been demonstrated that the pre-edge structures at the F-K edge result from hybridization with TM $3d$ states.[25] In the Zaanen-Sawatzky picture these metal states correspond particularly with $3d^{n+1}$ Hubbard band states.[28] Therefore, to be able to establish a direct comparison between these F-K pre-edge structures with the metal $3d$ band, a calculation in which only the $3d^{n+1}$ multiplet structure is present should help. To do so, we performed calculations of $2p$ to $3d$ absorption spectra with a $2p$ hole that does not interact with the $3d$ subshell and has no $2p$ spin-orbit interaction. We will refer to this $2p$ hole as a "$2p$ structureless hole." Technically, in the calculations we used the same parameters obtained to reproduce metal $L_{2,3}$ XAS spectra shown in Tables I and II, but we set the values of the Slater $F^k(2p;3d)$ and $G^k(2p;3d)$ integrals responsible for the $2p$-$3d$ Coulomb interaction and the metal $2p$ spin-orbit interaction equal to zero. The results are $2p$ absorption spectra containing only the multiplet structure of the $3d^{n+1}$ subshell in the presence of a structureless hole. Thus, the relative positions of the features in these simulated spectra give the multiplet structure of the $3d^{n+1}$ configuration. In order to compare these spectra with the fluorine K absorption spectra the multiplet energy must be shifted from the position of the center of gravity of the metal L edge to the fluorine K edge. It should be pointed out that in this calculation the intensities are given by the square of the $2p$ to $3d$ electric dipole transition matrix element. Therefore one does not expect the relative intensities in the fluorine K absorption spectra to follow the calculated intensities in this simplistic model.

IV. RESULTS AND DISCUSSION

A comparison between the measured TM $L_{2,3}$ absorption edges and the LFM calculation is shown in Fig. 1. For each compound the calculation gives all the $2p \rightarrow 3d$ electric dipole transitions that originate from the states thermally occupied in the $3d^n$ ground configuration. Each of these transitions is then convoluted with a Lorentzian that takes into account the effect of the $2p$ core hole width, and with a Gaussian function to simulate the monochromator contribution. There is very good overall agreement between experiment and theory for all compounds. The calculation predicts very well the peak energies and also in most cases the peak intensities. Characteristic increase in energy separation between L_3 and L_2 with the TM atomic number is evident. At this point it is clear that the major features in the metal $L_{2,3}$ absorption edge of the difluorides can be explained by the multiplet structure of the $3d^{n+1}$ configuration coupled to the $2p_j$ core hole without any need to include charge transfer effects.

In the case of Mn to Ni the calculation only includes the M^{2+} oxidation state for the transition metal, and therefore the interpretation of the spectra for these elements is straightforward. Here it is important to point out that steps in the intensity at both L_3 and L_2 edges were not subtracted from the experimental spectra, nor added to the calculated spectra. One therefore expects the calculated features to have lower intensity as the excitation energy progresses along each spectrum. In MnF_2 the calculation and the experiment are in remarkably good agreement. Later, for FeF_2 the agreement between our experiment and our calculation is not as good as for the other members of the MF_2 family. Basically the relative intensity of the transitions is not properly accounted for by our calculation. Despite this the agreement is fair. In CoF_2 the agreement is good, with the major discrepancy between experiment and theory at the Co L_2 edge, where theory predicts a dip in the cross section at about 793 eV and none is observed experimentally. Finally, for NiF_2 the agreement is good with the calculation accounting for the peak positions and intensities nicely. However, the width of the broad feature around 852 eV is not well reproduced by the calculation.

The agreement between experiment and theory is also very good for CrF_2. This must be contrasted with a previous attempt to model divalent Cr $2p$ XAS made by Theil *et al.*[9] In that work the best agreement with experiment was reached by considering D_{4h} symmetry with relatively large values of 10Dq and Ds (1.1 eV and 0.775 eV, respectively) while Dt was taken to be zero. However, their calculation failed to reproduce three distinctive sharp features located between L_3 and L_2 edges (see Fig. 1), which they incorrectly assumed as charge transfer features. More important, their calculation misled them to conclude that the ordering of the $3d$ orbitals changed.[9] This and the origin of the previously labeled charge transfer features will be clarified as we advance in the discussion of our results. As we can sense, CrF_2 was a particularly difficult compound to analyze since considering a nominal Cr^{2+} oxidation state does not give good results.[9] To address this problem, in our calculation we included Cr^+, Cr^{2+}, and Cr^{3+} oxidation states,

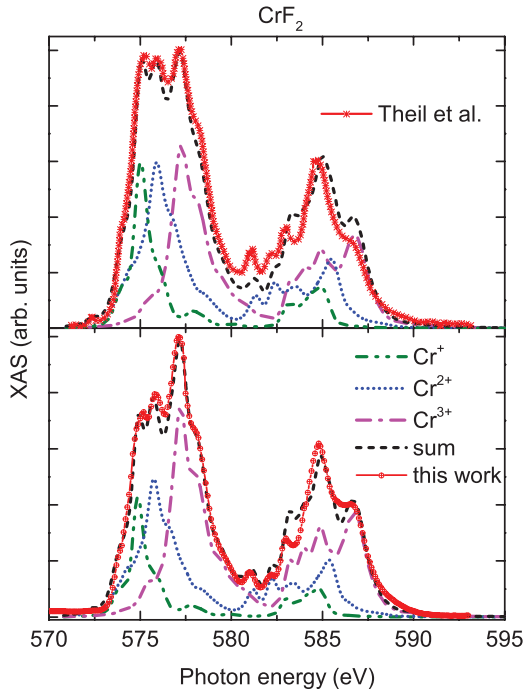

FIG. 2. (Color online) Comparison between the calculated and the experimental x-ray absorption spectra at the Cr $L_{2,3}$ edge. Bottom: this work; top: experimental spectrum from Theil *et al.*, Ref 9. The dash-double dotted (green), dotted (blue) and dash-dotted (magenta) lines are the contributions of Cr^{+}, Cr^{2+} and Cr^{3+}, respectively. The dashed (black) line is the sum of the three contributions. The linear superposition coefficients are given in Table II.

but with no need for large values of 10Dq or Ds (see Table II). By taking a linear superposition of absorption spectra for the three ions we were able to reproduce the main features in nominal CrF_2. A more detailed comparison between the experimental and the calculated spectra is shown at the bottom of Fig. 2. Here we subtracted the L_3 and L_2 steps from the data. In Fig. 2 we also show the individual contributions from each oxidation state, and the linear superposition obtained with the mixing coefficients given in Table II. It is clear that at both L_2 and L_3 edges there are contributions from all three ionic states, namely Cr^{+}, Cr^{2+}, and Cr^{3+}. As expected, the structures at both L edges correspond to Cr^{+}, then Cr^{2+}, and finally Cr^{3+} as the photon energy increases, but there are regions of overlap. There is now very good agreement between experiment and theory. The calculation accurately predicts the three sharp features between L_3 and L_2. The first two clearly belong to Cr^{2+}, while the third corresponds to a combination of all Cr^{+}, Cr^{2+}, and Cr^{3+}. The calculation overestimates the raise in absorption at this peak, but the agreement is otherwise rather good. For comparison, a digitalization of the CrF_2 absorption spectrum shown by Theil *et al.*[9] is presented in the top panel of Fig. 2. There was a discrepancy of about 0.8 eV between our energy scale and that of Ref. 9, so we decided to shift their data accordingly. Here the calculation includes absorption spectra for the same oxidation states, but with different mixing coefficients (see Table II) and a slightly larger instrument width. The agreement is again rather good. For this spectrum it is clear that there is a smaller relative contribution from Cr^{3+}. We therefore conclude that compared to previous results[7,9] our spectrum corresponds to a more oxidized sample. This can be seen in our spectrum as the peak at 577 eV (mostly Cr^{3+}) dominates over those at 575–576 eV (Cr^{2+}).

The comparison between experiment and theory allows a quantitative statement regarding the oxidation state of both samples. In our case we were dealing with $CrF_{2.26}$, while the sample in Ref. 9 corresponds to $CrF_{2.14}$. The presence of Cr^{+} and Cr^{3+} is most likely inherent to the synthesis process[33] due to disproportionation[28,29] from Cr^{2+} to Cr^{+} and Cr^{3+}. This can be concluded after our analysis and because even in the least oxidized spectrum for CrF_2 reported in literature there is a clear presence of Cr^{3+}.[7] Three different driving forces have been proposed to account for effective negative Hubbard U leading to disproportionation reactions in chemical species: (i) lattice distortions,[34] (ii) exchange correlation,[29] and (iii) strong hybridization with ligands.[28] Probably the three mechanisms are present at some degree in this material: Cr^{2+} has a $3d^4$ configuration and is therefore susceptible to Jahn-Teller distortion (this structural distortion was confirmed experimentally[35]), the magnetic exchange correlation mechanism was indeed proposed for Cr impurities in silicon, and as we demonstrated in this and in our previous work,[25] there is a significant degree of hybridization even in this extremely ionic family of materials. To address properly the mechanisms that drive disproportionation reactions in TM compounds and in chemical species, which is crucial for material sciences in general and for battery research in particular, requires a more detailed and systematic study that is beyond the scope of this work. However, resonant x-ray spectroscopies, particularly XAS and resonant inelastic x-ray scattering, can clearly help to unambiguously identify signatures of such processes and contribute to a better understanding of this crucial issue.

Once we have explained the origin of the structures in the TM $L_{2,3}$ XAS spectra, we will proceed to demonstrate that the pre-edge structures in the F-K spectra of the MF_2 display $3d$ TM multiplet effects. On the right side panels of Fig. 3 we present the absorption spectra obtained at the fluorine K edge. Compared to previous F-K XAS experiments we have found small discrepancies in the relative intensity of the F2p-TM3d hybridization features for the MnF_2 and FeF_2 spectra[4]. Such differences can be due to artifact effects and particularly for FeF_2 due to oxidation. This is possible since, as we mentioned before, we found this compound to be susceptible to oxidation. Additionally, the previously reported F-K FeF_2 spectrum seems to have a larger pre-edge intensity as compared to the other members of the MF_2 and MF_3 families also reported[4]. There is no apparent reason why this should be so. However, from our point of view these differences are only qualitative since they do not affect either the origin of the pre-edge structures nor their relative position, which are central topics in our discussion. For all compounds the spectra can be divided in two regions. The first is comprised from 690 to 700 eV of structures similar and common to all the difluorides. The broad structures observed here are associated with excitation into unoccupied F 2p orbitals hybridized with the TM 4s, 4p orbitals. The second region, where main differences among the spectra occur, corresponds to the pre-edge below 690 eV. Here, distinctive features vary drastically from one compound to the next. These structures have been assigned to the progressive filling of M 3d (e_g or t_{2g}) orbitals hybridized to F (ligand) 2p

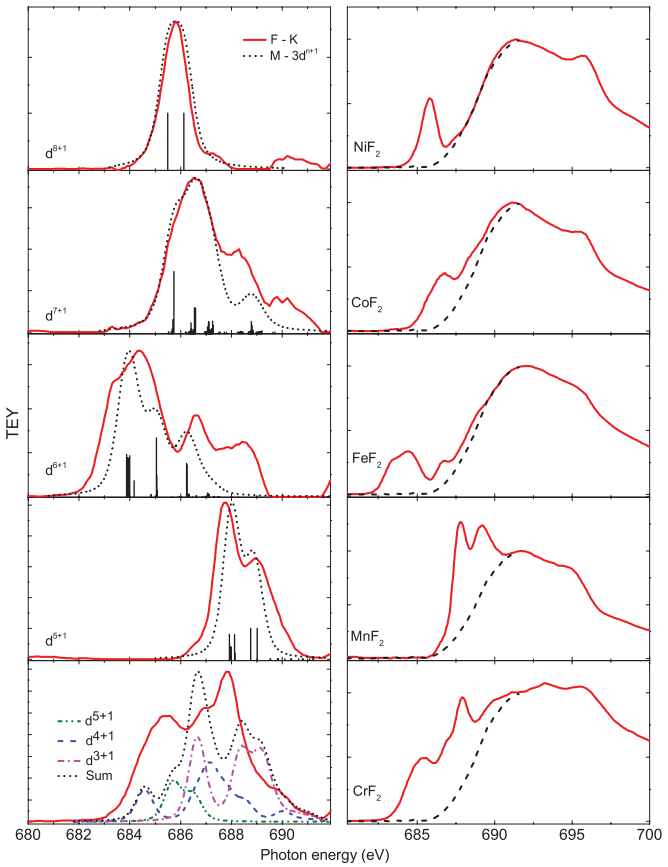

FIG. 3. (Color online) Right side column: Experimental TEY spectra obtained at the fluorine K edge (red solid line), the black dashed line is the edge to be subtracted (see text for details). Left side column: Expansion at the pre-edge of fluorine K edge after edge subtraction. Black dotted lines are the convoluted d^{n+1} states (black vertical bars) for TM^{2+} cations with d^n electron count.

empty states.[6] Changes in their relative intensity along the $3d$ transition metal series has been used to assign qualitatively the $3d$ spin up or down sub-bands.[4] However, only recently the variation of the onset energy of these hybridization features has been fully addressed.[25]

Although it is known that those structures appear due to TM$3d$-F$2p$ hybridization and their shape is directly related to TM $3d$ states, it is not self evident how they can be observed in the pre-edge of F-K XAS spectra. In the simplistic description, during the x-ray absorption at the F-K edge, a $1s$ F electron is promoted to F $2p$ unoccupied states. Once in the $2p$ conduction band, due to hybridization, there is a probability that this electron will be partially localized in the vicinity of the $3d$ sub-bands. Because of this, aside from the attractive effect of the F $1s$ core hole left behind, this electron will experience the interactions inherent to $3d$ shell electrons: Coulomb $3d$-$3d$, $3d$-spin orbit, as well as the crystal field exerted by surrounding F ions. So by the x-ray absorption process at the F-K edge we are actually indirectly probing the $3d$ shell and the interaction that $3d$ electrons experiment by the inclusion of an extra $3d$ electron. We performed atomic multiplet calculations including the interactions mentioned above for the cations with an additional $3d$ electron. In this manner we ended having a $3d^{n+1}$ configuration for each cation. Interestingly, as we will show below, the agreement between our calculated results and the pre-edge structures in F-K XAS spectra is good. In most of the cases the calculation correctly accounts for the number of structures but slightly fails in estimating the energy separation among them and their relative intensity as compared to those observed in the spectra. This result is surprising considering the simplistic model followed in this work to capture evidence of the TM$3d$-F$2p$ hybridization process.

At this moment it is convenient to connect our approach to one of the most important qualitative ideas in the theory of correlated electrons: upper (d^{n+1}) and lower Hubbard (d^{n-1}) Bands of a d^nsystem. In the Hubbard model these bands arise when polarity fluctuations of the type $d_i^n d_j^n \rightarrow d_i^{n-1} d_j^{n+1}$(where i and j label different sites and n is the d orbital occupation) are suppressed. This gives birth to a correlation band gap and occurs when the Coulomb and exchange energies (U) associated to them are larger than the one-electron dispersional bandwidth.[36] The magnitude of this Hubbard U can be determined from the energy separation between the gravity centers[25,28] (or between lowest energy multiplets[1,37]) of the d^{n-1} and d^{n+1} TM configurations. In the Zaanen-Sawatzky-Allen model, which is an ionic model, they are calculated starting from an atomic description that later includes crystal (Madelung energies, crystal fields) and band effects (bandwidth, polarization, screening).[28] The pre-edge structures in F-K spectra are no doubt UHBs from the metals which are observed due to F$2p$-TM$3d$ hybridization, or more precisely, with d^{n+1} states.[25] Since our calculations of $3d^{n+1}$ states do not include any hybridization term, solid, or band corrections, they are not those of an UHB. Although configuration-interaction cluster calculations[26] and time dependent DFT calculations[2] are in principle better suited to describe ligand $2p$-TM $3d$ hybridization in ligand K edge XAS, only the first can account for multiplet effects. In this sense, relatively simpler calculations like the ones presented here directly give the structure of the d^{n+1} TM multiplet regardless of the origin of the extra d electron.

On the left side panels of Fig. 3 we compare the F-K pre-edge structure with the results of the structureless $2p$ hole calculation. To isolate the pre-edge structure in the experimental data we subtracted the edge indicated by the dashed lines in the right hand panels. This edge was the same for all spectra and was obtained by the following procedure. First all spectra were normalized so that they had the same intensity at the local maximum at about 691 eV. On the low energy side, below 685 eV, the edge was chosen as the lowest of the absorption spectra, which clearly corresponds to MnF_2. In the region between 688 and 691 eV the edge is also given by the lowest of the absorption spectra, which now corresponds to FeF_2 and NiF_2. Finally, the edge values between 685 and 688 eV were obtained by a cubic spline interpolation connecting these low and high energy segments. The resulting pre-edge structures shown in red solid lines on the left side panels of Fig. 3 are the difference between the experimental absorption spectra and this common edge. They are now compared with the results of the structureless $2p$ hole calculated spectra (dotted line). For these we used the same widths as the ones used for the $L_{2,3}$ calculations in Fig. 1.

In the case of nominal CrF_2, calculations of d^{n+1}states for Cr imply a d^{3+1} (magenta dot-dashed line), a d^{4+1} (blue

dashed line), and a d^{5+1}(green short dashed line) configuration corresponding to Cr^{3+}, Cr^{2+} and Cr^{+}, respectively. The sum spectrum (black dashed line) is the sum of the three individual spectra, with the proportion given by the superposition coefficients in Table II. The comparison was made by shifting the maximum in the sum spectrum to match the experimental peak at 687 eV, then all the components were shifted by the same value. Notice that the maximum in the sum corresponds to the maximum in d^{3+1} Cr^{3+}, and also that the minimum energy peak just below 685 eV belongs to the d^{4+1} multiplet. Interestingly, all the other features in the calculation align naturally with the experimental ones. It is also remarkable that the measured relative intensities are not very far off the sum calculated in this very simplistic approximation. In this way, all features of the F-K pre-edge in CrF_2 are explained.

For MnF_2 we see that the d^{5+1}calculation for Mn^{2+} shows two main structures which once shifted resemble nicely the experimentally observed doublet. In the case of FeF_2, we present a d^{6+1}calculation for Fe^{2+}. Clearly the calculation predicts the number of structures and accounts relatively well for their energy separation but fails in reproducing their relative intensity. In the case of CoF_2, the results for a d^{7+1} configuration in Co^{2+} are shown. Here the calculation predicts four main structures. The first two seem to match the F-K pre-edge while the third and fourth may be obscured by the raising of the Co 4*s*,4*p* band. Finally, on top of Fig. 3 the result for d^{8+1} in NiF_2 is shown. In Ni we only see one peak and therefore the calculation can be shifted to match the main feature observed in the experimental result. However the small shoulder at 687 eV cannot be explained within this simple model. As we have shown, although our M^{2+} d^{n+1} calculations cannot explain all the structures of the F-K pre-edge spectra they follow nicely the experimental results.

Experimentally a direct method for identifying the origin of the rich pre-edge structures on ligand K edge spectra, without theoretical aid, is desirable. In Fig. 4 we shifted each TM L_2 and L_3 spectra in energy, up for Cr and Mn and down for all the others, until their structures were aligned with those observed at the F-K edges for each compound. Notice that under this reasoning we could also have proceeded by shifting the F-K edge spectra for each compound to the respective metal $L_{2,3}$ spectra. For completeness we also show the corresponding spectra for CuF_2. The intensity scale of all spectra was adjusted so that a direct comparison can be made. It is clear that the major changes in the F-K edge occur in the same energy interval covered by both TM L_3 or L_2 edges. Furthermore, a one to one correspondence between features in both spectra can be made although the TM structures are somehow smeared by the convolution of the broader F 2*p* band.

In CrF_2, what appears as a doublet in the metal L_3 edge corresponds with the first broad maximum in fluorine (685.5 eV); this doublet structure is not resolved because of the different inherent bandwidths for TM 3*d* and F2*p* bands, estimated in ≈0.5 eV and 3–4 eV, respectively.[28] From Fig. 2 it is clear that these structures in Cr L_3 arise mostly from Cr^{+} and Cr^{2+} multiplet states. The peak of maximum intensity at the Cr L_3 edge can be aligned with the shoulder around 687 eV in the fluorine spectrum. We have shown that this peak on CrF_2 L_3 originates mostly from Cr^{3+} with some contribution from Cr^{2+} multiplets (see Fig. 2). With this alignment, the

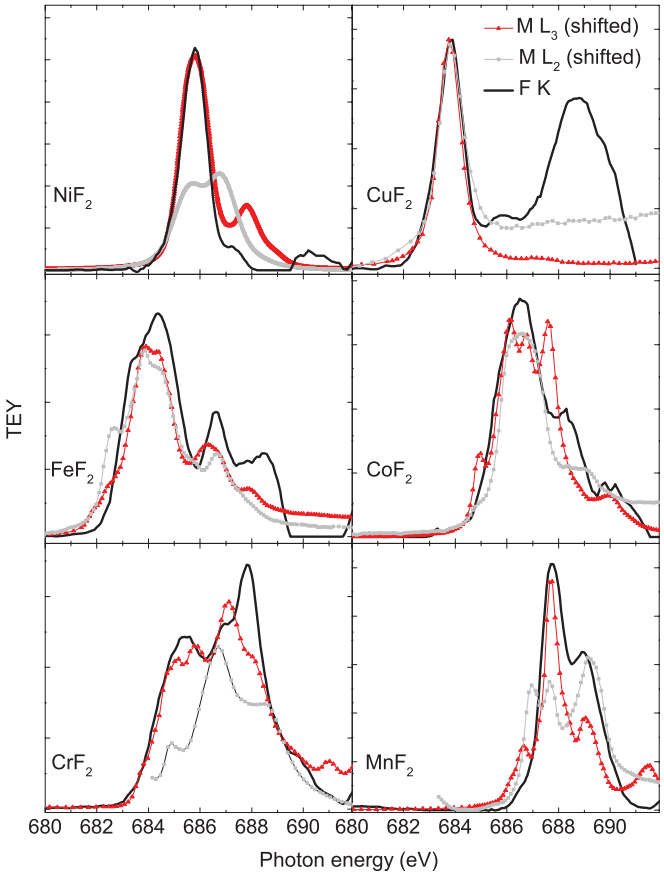

FIG. 4. (Color online) Comparison between metal $L_{2,3}$ absorption edges and F-K pre-edge structures. Black solid lines: F-K pre-edge structures. Red triangles and gray squares are, respectively, metal L_3 and metal L_2 edges from the corresponding metal XAS spectra.

highest energy shoulder in the Cr L_3 spectrum aligns nicely with the prominent F-K peak at 688 eV. When we proceed to compare L_2 structures with the F-K pre-edge, the analysis is not direct. This occurs because it is not obvious where the L_2 edge starts due to the presence of multiplet structures of Cr^{+}, Cr^{2+}, and Cr^{3+} between the main L_3 and L_2 edges. The alignment of Cr L_2 to the F-K pre-edge was made considering the rise in the experimental Cr spectrum at approx 582.5 eV as the beginning of L_2. In this way the main L_2 peak in Cr, which has both Cr^{2+} and Cr^{3+} contributions, aligns with the first F-K pre-edge structure. On the other hand, the high energy shoulder at L_2, with mostly Cr^{3+} character, aligns properly with the second F pre-edge structure at 687 eV. Therefore this empirical method can be used to unambiguously align the structures on the F-K pre-edge with those from Cr regardless of its oxidation state.

In the case of MnF_2, the first metal L_3 edge structure aligns well with that of the F-K pre-edge at 686.5 eV. The next two major peaks in manganese have corresponding, broader absorption peaks in fluorine at about 688 and 689 eV. The Mn L_2 portion of the spectrum has three main features which align accordingly with corresponding F-K pre-edge features. The smallest 3*d* contribution compared to the metal 4s, 4p intensity occurs for FeF_2 (see Fig. 3), and even in this case the

shoulder at 687 eV is aligned with absorption features in both metal L_3 and L_2 edges. Here it is worth mentioning that a gain in the intensity of the high energy shoulder in the leading edge of the F-K spectrum (≈684 eV) correlates with the raising of an oxidation peak in Fe^{2+} (≈709 eV in Fig. 1). This peak in Fe^{2+} increased its intensity with time even with the sample inside the ultrahigh vacuum chamber. At the end we ended up with Fe $L_{2,3}$ spectra similar to those reported by Krasnikov *et al.*[17] For CoF_2 there is a good correspondence between features in both Co $L_{2,3}$ and F-K spectra. This is especially true for the better resolved L_3 portion, where the first three peaks align under the broad F-K pre-edge structure. The high energy shoulders at L_3 also seem to align with the structures on the raising $4s$,$4p$ band, especially that at 688.5 eV. In the case of NiF_2, the second peak in the Ni $L_{2,3}$ doublet has a corresponding shoulder at the sharp rise in the hybridized fluorine-nickel $4s$,$4p$ portion of the spectrum (≈687 eV). This shoulder does not exist in the comparable F-K spectrum of CuF_2 because in this case the transition leaves the $3d$ shell completely occupied. As we have shown, this empirical procedure allows us to account for most of the structures on the F-K pre-edges. This is both useful and surprising considering the physics involved, namely that multiplet effects of the metal manifest themselves on the F-K pre-edges in XAS. We argue that this is the case given the clear origin of the structures on the TM $2p \rightarrow 3d$ spectra and their mirrors observed at the F-K pre-edge spectra.

In oxides the relative intensity of $2p$-$3d$ hybridized states diminishes with the availability of holes in the $3d$ bands.[3] We do not observe that behavior at the F-K edge in MF_2. For these compounds the relative intensity of these states to the $4s$,$4p$ bands is relatively constant but significantly smaller than those in oxides.[1–3] This loss in relative intensity has been attributed in d^5 and d^6 oxides to a decrease in the strength of the hybridization of T$M3d$-O$2p$ due to the shrinking of the metal $3d$ orbitals in late $3d$ metals. The fact that the relative intensity of the leading edges to the $4s$,$4p$ bands is smaller in difluorides as compared to oxides is evidence of weaker hybridization strength in difluorides as compared to the more covalent oxides. This scenario is consistent with the strong ionic bonding picture in difluorides. The connection of the multiplet structures from the metal at the F-K edge is clearer in MF_2 as compared to oxides because of the strong ionic character of the difluorides, the narrowing of the F $2p$ band as compared to that of oxygen due to the increase in the effective nuclear charge, and the decrease in the atomic radii.

V. CONCLUSIONS

We presented a detailed and systematic study of the metal $L_{2,3}$ and the fluorine K absorption edges of the TM difluorides. Through our LFM $2p \rightarrow 3d$ calculations on TM ions we demonstrated that the deviation of O_h symmetry is small in this family of compounds, even for the archetypical Jahn-Teller distorted CrF_2. We were able to solve a long standing issue on the interpretation of Cr $L_{2,3}$ XAS spectrum in CrF_2 identifying its structures by considering the presence of Cr^+, Cr^{2+}, and Cr^{3+} in the sample. LFM calculations for TM with $3d^{n+1}$ configurations with a $2p$ core hole without any structure were performed to explain $3d$-$2p$ hybridization features in F-K spectra. We found good agreement after comparison with experimental results. We propose a useful and accurate empirical method for identifying $3d$-$2p$ hybridization features in K edge spectra of ionic systems by direct comparison with metal $L_{2,3}$ edges. We argue that the $2p$-$3d$ hybridization structures at the ligand K edge in ionic systems, which directly give the TM UHBs,[25] also contain structures that mirror the TM $L_{2,3}$ atomic multiplets.

ACKNOWLEDGMENTS

P.O.V. would like to acknowledge support from Centro de Ciencias de la Complejidad-UNAM and ALS-SSG during partial preparation of this manuscript. The Advanced Light Source is supported by DOE(DE-AC03-76sF0009). P.O.V. and J.J.M. would like to thank the support of CONACyT México, respectively, under postdoctoral scholarship and under research Grant No. 56764.

*paulolalde@gmail.com
†jimenez@nucleares.unam.mx

[1] F. de Groot and A. Kotani, *Core Level Spectroscopy of Solids* (CRC Press, Boca Raton, Florida, 2008).
[2] S. G. Minasian, J. M. Keith, E. R. Batista, K. S. Boland, J. A. Bradley, S. R. Daly, S. A. Kozimor, W. W. Lukens, R. L. Martin, D. Nordlund, G. T. Seidler, D. K. Shuh, D. Sokaras, T. Tyliszczak, G. L. Wagner, T.-C. Weng, and P. Yang, J. Am. Chem. Soc. **135**, 1864 (2013).
[3] F. M. F. de Groot, M. Grioni, J. C. Fuggle, J. Ghijsen, G. A. Sawatzky, and H. Petersen, Phys. Rev. B **40**, 5715 (1989).
[4] A. S. Vinogradov, S. I. Fedoseenko, S. A. Krasnikov, A. B. Preobrajenski, V. N. Sivkov, D. V. Vyalikh, S. L. Molodtsov, V. K. Adamchuk, C. Laubschat, and G. Kaindl, Phys. Rev. B **71**, 045127 (2005).
[5] S. Nakai, K. Ogata, M. Ohashi, C. Sugiura, T. Mitsubishi, and H. Maezawa, J. Phys. Soc. Jpn. **54**, 4034 (1985).
[6] S. Nakai, A. Kawata, M. Ohashi, M. Kitamura, C. Sugiura, T. Mitsuishi, and H. Maezawa, Phys. Rev. B **37**, 10895 (1988).
[7] C. T. Chen and F. Sette, Physica Scripta **T31**, 119 (1990).
[8] A. Tanaka and T. Jo, J. Phys. Soc. Jpn. **61**, 2040 (1992).
[9] C. Theil, J. van Elp, and F. Folkmann, Phys. Rev. B **59**, 7931 (1999).
[10] J. Jiménez-Mier, D. L. Ederer, and T. Schuler, Phys. Rev. B **70**, 035216 (2004).
[11] J. Jiménez-Mier, D. L. Ederer, and T. Schuler, Phys. Rev. A **72**, 052502 (2005).
[12] F. M. F. de Groot, J. C. Fuggle, B. T. Thole, and G. A. Sawatzky, Phys. Rev. B **42**, 5459 (1990).
[13] F. M. F. de Groot, J. Electron Spectrosc. Relat. Phenom. **67**, 529 (1994).
[14] F. M. F. de Groot, Coord. Chem. Rev. **249**, 31 (2005).
[15] F. de Groot, Chem. Rev. **101**, 1779 (2001).
[16] C. Sugiura, J. Phys. Soc. Jpn. **60**, 2710 (1991).

[17]S. A. Krasnikov, A. S. Vinogradov, A. B. Preobrajenski, L. K. Gridneva, S. L. Molodtsov, C. Laubschat, and R. Szargan, Physica Scripta **T115**, 1074 (2005).
[18]F. M. F. de Groot, J. Faber, J. J. M. Michiels, M. T. Czyzyk, M. Abbate, and J. C. Fuggle, Phys. Rev. B **48**, 2074 (1993).
[19]S. P. Kowalczyk, L. Ley, F. R. McFeely, and D. A. Shirley, Phys. Rev. B **15**, 4997 (1977).
[20]E. I. Esmail and D. S. Urch, Spectrochim. Act. **39A**, 573 (1983).
[21]A. S. Koster, J. Phys. Chem. Solids **32**, 2685 (1971).
[22]P. Dufek, P. Blaha, V. Sliwko, and K. Schwarz, Phys. Rev. B **49**, 10170 (1994).
[23]H. Das, S. Kanungo, and T. Saha-Dasgupta, Phys. Rev. B **86**, 054422 (2012).
[24]I. P. R. Moreira, R. Dovesi, C. Roetti, V. R. Saunders, and R. Orlando, Phys. Rev. B **62**, 7816 (2000).
[25]P. Olalde-Velasco, J. Jiménez-Mier, J. D. Denlinger, Z. Hussain, and W. L. Yang, Phys. Rev B **83**, 241102(R) (2011).
[26]J. van Elp and A. Tanaka, Phys. Rev. B **60**, 5331 (1999).
[27]S. D. George, P. Brant, and E. I. Solomon, J. Am. Chem. Soc. **127**, 667 (2004).
[28]J. Zaanen and G. A. Sawatzky, J. Sol. State. Chem. **88**, 8 (1990).
[29]H. Katayama-Yoshida and A. Zunger, Phys. Rev. Lett. **55**, 1618 (1985).
[30]J. J. Jia, T. A. Callcott, J. Yurkas, A. W. Ellis, F. J. Himpsel, M. G. Samant, J. Stöhr, D. L. Ederer, J. A. Carlisle, E. A. Hudson, L. J. Terminello, D. K. Shuh, and R. C. C. Perera, Rev. Sci. Instrum. **66**, 1394 (1995).
[31]M. O. Krause and J. H. Oliver, J. Phys. Chem. Ref. Data **8**, 329 (1979).
[32]E. Stavitski and F. M. F. de Groot, Micron **41**, 687 (2010).
[33]B. J. Sturm, Inorg. Chem. **1**, 665 (1962).
[34]P. W. Anderson, Phys. Rev. Lett. **34**, 953 (1975).
[35]J. W. Cable, M. K. Wilkinson, and E. O. Wollan, Phys. Rev. **118**, 950 (1960).
[36]J. Hubbard, Proc. R. Soc. London A **277**, 237 (1964); **281**, 401 (1964).
[37]A. Fujimori, A. E. Bocquet, T. Saitoh, and T. Mizokawa, J. Electron Spectrosc. Relat. Phenom. **62**, 141 (1993).